Simulating idealized Dansgaard-Oeschger events and their potential impacts on the global methane cycle

Peter O. Hopcroft [a,*], Paul J. Valdes [a], David J. Beerling [b]

[a] Bristol Research Initiative for the Dynamic Global Environment (BRIDGE), School of Geographical Sciences, University of Bristol, Bristol, BS8 1SS, UK
[b] Department of Animal and Plant Sciences, University of Sheffield, Sheffield, S10 2TN, UK

ARTICLE INFO

ABSTRACT

Ice-core records indicate that during the last glacial period, atmospheric CH_4 and Greenland temperature rose abruptly in a series of Dansgaard-Oeschger (D-O) events. These increases attained up to two-thirds of the glacial-interglacial amplitude for CH_4. We use these major changes as possible constraints on the mechanisms of D-O variability. A series of simulations are performed with a coupled atmosphere-ocean general circulation model with a time-dependent freshwater forcing which induces rapid variations in the Atlantic meridional overturning circulation (AMOC). The transient climate output is then used to drive a dynamic vegetation model which simulates wetland CH_4 emissions. During freshwater input, emissions are reduced and, in sensitivity simulations, demonstrate strong dependence on the background climate (orbital insolation or ice sheet extent). In the reverse situation, the strengthening of the AMOC leads to warming over Northern Eurasia, but only minor change to the hydrological cycle in the tropics where most CH_4 emissions occur. This is a robust result from the climate models examined and is of central importance to our results, which suggest that AMOC driven CH_4 variations are considerably smaller than observed D-O events. Modelled emissions of volatile organic compounds (VOC) lead to a significant effect on the CH_4 lifetime during these events, but both the VOC emissions model and VOC effects on CH_4 lifetime are subject to uncertainty. The model results can only be reconciled with some of the larger changes in the ice-core record by including the effect of VOCs and by taking the total amplitude of AMOC perturbation from weak to very strong. Our results suggest that either the model is too insensitive to change, or that further mechanisms may be important for the large CH_4 changes during D-O events. In particular, a strengthening of the AMOC alone cannot reproduce the observed abrupt CH_4 increases. Comparisons with independent models would help to identify possible avenues for further work.

© 2011 Elsevier Ltd. All rights reserved.

1. Introduction

CH_4 is an important atmospheric trace gas which contributes significantly to the planetary greenhouse effect. The concentration of CH_4 in the atmosphere has risen sharply since the beginning of the industrial era and is thought to have contributed approximately 18% of the direct, increased greenhouse gas radiative forcing over this time period (Forster et al., 2007). Changes in both CH_4 sources (e.g. wetlands, biomass burning, agriculture) and sinks (e.g. reaction with the hydroxyl radical OH, or oxidation in soils) are responsible for atmospheric CH_4 levels at a given time. CH_4 concentrations therefore act as a global signature of biogeochemical cycles, and reveal information about the climatic state. Given the

likely contribution to future climatic warming, an understanding of how natural sources of CH_4 behave under rapidly changing climate is imperative.

Reconstructions from polar ice cores show that CH_4 concentrations [CH_4] have varied greatly in concert with past climate. During successive glacial and interglacial stages of the past 800 kyr, the CH_4 concentration varied between approximately 350 ppbv (parts per billion by volume) and 650 ppbv. The reduction during glacial periods is thought to result primarily from the large scale cooling which has a direct negative impact on emissions (Kaplan, 2002; Valdes et al., 2005). The atmospheric CH_4 budget was additionally thought to be affected by an increase in the oxidative capacity of the atmosphere at the LGM, mostly as a result of decreased emissions of volatile organic compounds (VOC) from vegetation.

The climate of the last glacial (and previous glacial epochs) was characterised by striking variability with a millennial time-scale

* Corresponding author. Tel.: +44 117 33 18352.
E-mail address: peter.hopcroft@bris.ac.uk (P.O. Hopcroft).

(e.g. Dansgaard et al., 1993; NGRIP Project Members, 2004; Wolff et al., 2010), the most prominent feature of which is a series of abrupt jumps in Greenland temperature of between 8 °C and 16 °C over the course of a few decades. These abrupt warming events, or Dansgaard-Oeschger (D-O) events, also have counterparts in the ice-core records of CH_4 (as well as accumulation, dust and N_2O), with CH_4 jumps of up to two-thirds the glacial-interglacial concentration change, achieved in a few decades (Chappelaz et al., 1993; Blunier and Brook, 2001; Flückiger et al., 2004; Huber et al., 2006, Fig. 1). This implies a tight (although temporally variable) coupling between the climate changes associated with D-O warming events and the global biogeochemical cycles which are responsible for CH_4 concentrations in the pre-anthropogenic Earth system.

The role of the Atlantic meridional overturning circulation (AMOC) in abrupt climate change was originally proposed by Broecker et al. (1985) amongst others, and has gained support in a number of modelling and proxy studies (Ganopolski and Rahmstorf, 2001; Clark et al., 2002; McManus et al., 2004; Schmittner and Galbraith, 2008; Liu et al., 2009). Changes in AMOC are thought to lead to variations in the amount of the heat transported northwards in the Atlantic Ocean and in the position or strength of the inter-tropical convergence zone (ITCZ) both on an inter-annual time-scale and in past climates (e.g. Peterson et al., 2000; Wang et al., 2004). Abrupt rises in CH_4 have been attributed to increasing temperatures in the NH extra-tropical regions brought about by AMOC variations (Dällenbach et al., 2000; Fischer et al., 2008; Bock et al., 2010). However, causative mechanisms of D-O events remain poorly understood, and global climatic signatures are only sparsely resolved.

Here, we investigate the possible constraints that can be placed on D-O behaviour and natural, abrupt CH_4 variations, by using a comprehensive Earth system modelling framework. We simulate both climate and wetland CH_4 emissions by forcing a coupled general circulation model with idealized freshwater perturbations over the North Atlantic ocean. We attempt to replicate the large changes of temperature and CH_4 evident in the ice-core record.
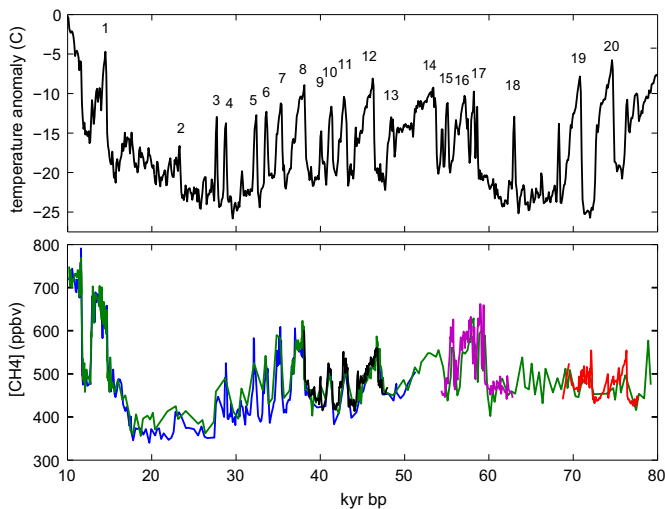
Fig. 1. Greenland temperature anomaly from present derived from GRIP ice-core data (Masson-Delmotte et al., 2005) and CH_4 (Blunier and Brook, 2001; Flückiger et al., 2004; Huber et al., 2006) from Greenland on the GICC05 time-scale (from Wolff et al., 2010). Dansgaard-Oeschger events 1−20 are labelled. Colours correspond to different ice-core records. (For interpretation of the references to colour in this figure legend, the reader is referred to the web version of this article.)
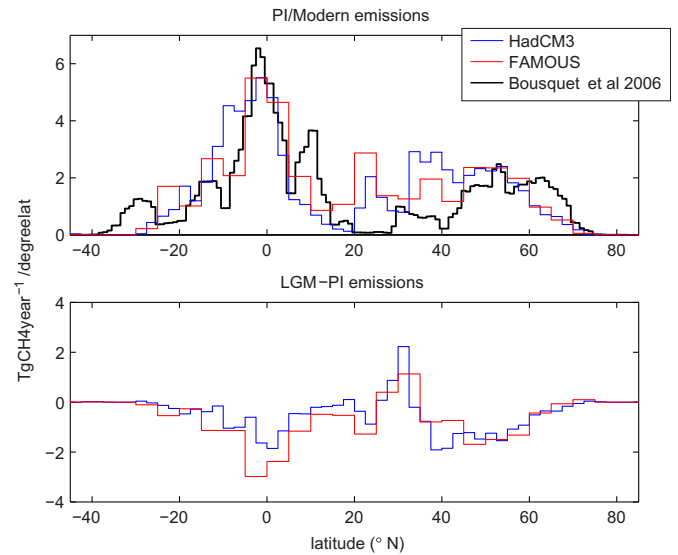

Fig. 2. Top: wetland CH_4 emissions for pre-industrial simulations with HadCM3 and FAMOUS and mean AD 1984−2005 emissions from Bousquet et al. (2006). Bottom: the change in emissions at the LGM for HadCM3 and FAMOUS.

2. Methods

2.1. Climate model

We use the FAst Met Office UK Universities Simulator (FAMOUS), a coupled general circulation model (Jones et al., 2005; Smith et al., 2008) which is a low-resolution version of the UK Met Office's HadCM3 (Gordon et al., 2000). FAMOUS was originally tuned to mimic the climate simulation of HadCM3 (Jones et al., 2005), but more recent modifications, particularly of the ozone and sea-ice parameterisations, have improved the climatology of high-latitudes by removing a significant cold bias and an overestimate of the Arctic sea-ice area (Smith et al., 2008).

FAMOUS consists of a 3D hydrostatic, primitive equation, grid point atmospheric general circulation model with a resolution of 7.5° in longitude and 5.0° in latitude, with 11 unequally spaced levels in the vertical. Land processes are simulated at the same
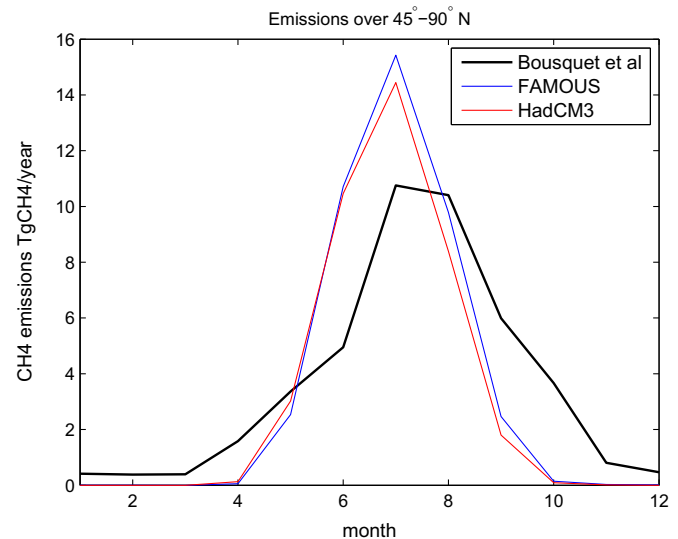
Fig. 3. Monthly pre-industrial emissions averaged northwards of 45°N for FAMOUS, HadCM3 and derived from 1984 to 2005 average of the Bousquet et al. (2006) data.

resolution as the atmospheric GCM using the MOSES1 scheme (Cox et al., 1999). The ocean component is the HadOM3 model (Gordon et al., 2000), a primitive equation 3D model, with a rigid lid formulation. It has a horizontal resolution of $3.75°$ in longitude and $2.5°$ in latitude, with 20 unequally spaced levels in the vertical. The sea-ice model uses zero-layer thermodynamics with parametrizations of ice drift and leads (Cattle and Crossley, 1995). The atmosphere and ocean are coupled once a day. A fractional land sea mask is used in order to account for the differing grids used in the atmosphere and ocean components. FAMOUS does not require any artificial heat or momentum fluxes in order to simulate a stable climate. A small freshwater correction is applied over ocean areas close to present day ice sheets. This is used to account for iceberg calving and hence conservation of global water volume, since ice flow is not explicitly represented within the model. FAMOUS runs at around 100 years per day of computation when distributed on 8 processors.

2.2. Methane and VOC emission models

We force the Sheffield Dynamic Global Vegetation Model (SDGVM) (Woodward et al., 1995; Beerling and Woodward, 2001) with output climatology from the GCM as in the work of Valdes et al. (2005) and Singarayer et al. (2011). SDGVM calculates the transient evolution of the global distribution of vegetation functional types, net primary productivity and canopy structure as well as soil water content. These are used to drive a model of global wetland distribution and anaerobic microbial CH_4 production and aerobic CH_4 oxidation (Cao et al., 1996) and a model of volatile organic chemical (VOC) emissions (Guenther et al., 1995). Both SDGVM and the emissions models are configured at the same resolution as the atmospheric component of FAMOUS.

The wetland model has been modified to predict the seasonally varying spatial distribution of wetlands based on the input climate variables and soil water content as simulated by SDGVM. The SDGVM soil hydrology model calculates the soil moisture profile to a depth of 1 m using 4 layers with the surface layer of thickness 5 cm and the remaining three of equal depth. Each of the four bucket levels has a field capacity and wilting point which define the minimum and maximum water storage capacity. Once a layer is at the maximum limit, further water is transferred to the lower level. If all four levels are at field capacity, any further water leads to runoff. Two further moisture storage pools representing liquid and frozen snow are additionally simulated. Bare soil evaporation, sublimation, transpiration and interception are incorporated. Transpiration occurs in each level and is weighted by the root density and the wilting point. The hydrology model is run on a daily timestep. When temperatures are sub-zero, all precipitation is taken as snow. When the temperature exceeds zero, frozen snow is melted to form snow melt at a rate proportional to the temperature (in Celsius). Precipitation and any snow melt then enter the uppermost bucket level. The monthly average values of soil water content are then used to calculate monthly water table positions using the relations defined in Cao et al. (1996). Here both inundated and non-inundated wetlands as in Cao et al. (1996) are considered, with the cutoff defined as being when the water table position is 10 cm above the soil surface.

Methanogenesis is assumed to be limited by evapotranspiration in non-seasonally frozen environments. Thus in the tropics, emissions only occur when precipitation exceeds evapotranspiration. The latter is calculated with the Penman–Monteith equation (Monteith and Unsworth, 1990) using climate variables simulated in the GCM. Four factors then determine the rate of CH_4 emissions: temperature, soil organic matter respiration, water table depth and vegetation productivity (Cao et al., 1996). Emissions are assumed to

be zero if the temperature is at or below 5 °C and if the water table drops more than 10 cm below the soil surface. The VOC emission model (Guenther et al., 1995) takes account of leaf area index simulated by SDGVM in addition to temperature and incident solar radiation simulated in the climate model. Both the CH_4 and isoprene emissions are integrated over each grid-box (at the GCM resolution), which in FAMOUS is additionally multiplied by the fractional land sea mask so that the total land area is realistic. A correction is also made using sub-grid orographic variance so that CH_4 emissions are reduced where the variance is larger (Valdes et al., 2005), given that wetlands typically occur in areas of reduced orographic gradients.

This coupled Earth System modelling approach successfully simulated the large CH_4 variations that occur between the Last Glacial Maximum and pre-industrial climates (Valdes et al., 2005), as well as the pre-industrial Holocene variations (Singarayer et al., 2011). These studies used a higher resolution version of the climate model and so in Section 3.1 we compare the CH_4 emissions simulated by FAMOUS and with the higher-resolution model HadCM3.

2.3. D-O event simulations

Our baseline climate simulation is representative of the last glacial maximum (LGM), and is forced with boundary conditions following the Paleoclimate Model Intercomparison Project protocol (Braconnot et al., 2007, http://pmip2.lsce.ipsl.fr/). This specifies 21 kyr orbital configuration, reduced atmospheric concentrations of major greenhouse gases (CO_2: 185 ppmv, CH_4: 355 ppbv and N_2O: 245 ppbv), 21 kyr glaciation extent (Peltier, 2004), and a lowering of sea level by 120 m which leads to increased land area. Our simulation predicts a global LGM cooling from the pre-industrial simulation of 4.7 °C, consistent with other model estimates (Braconnot et al., 2007). The LGM Atlantic MOC is stable, with a mean value of 19.6 Sv (1 Sv = 1×10^6 m^3 s^{-1}) versus a value of 17.5 Sv in the pre-industrial simulation. Sea-ice reaches further south in the LGM simulation, and the main region of deep convection in the North Atlantic is shifted southwards towards the location of Iceland.

We also analyse a series of sensitivity experiments in order to begin to explore how the D-O events might have responded to changes in climatic conditions which occurred through the last glacial cycle. In these simulations, one or more of the climatic boundary conditions are modified. In particular we additionally used pre-industrial ice sheets (from Peltier, 2004) and atmospheric CO_2 levels as well as a modified orbital insolation pattern that corresponds to a precessional minimum.

In all simulations freshwater forcing is applied as a virtual salinity flux due to the rigid lid approximation of the ocean model. In these experiments the flux is applied in the zonal band from 50° to 70°N over the Atlantic Ocean at a maximum rate of 0.5 Sv (1 Sv = 1×10^6 m^3 s^{-1}) which equates to a global sea level equivalent change of approximately 4 m per century. In all experiments the forcing is applied as a freshwater input followed by an evaporative flux. This second step produces a rapid reinvigoration of the AMOC (e.g. Schmittner and Galbraith, 2008), which leads to a rapid warming in the region of the North Atlantic. As the forcing is relaxed the model tends to the initial, unperturbed state. This forcing is shown in Fig. 4.

3. Results

3.1. Model behaviour and evaluation

We first compare the effects of pre-industrial and glacial (LGM) climatic forcings on the simulated emissions of CH_4. We compare
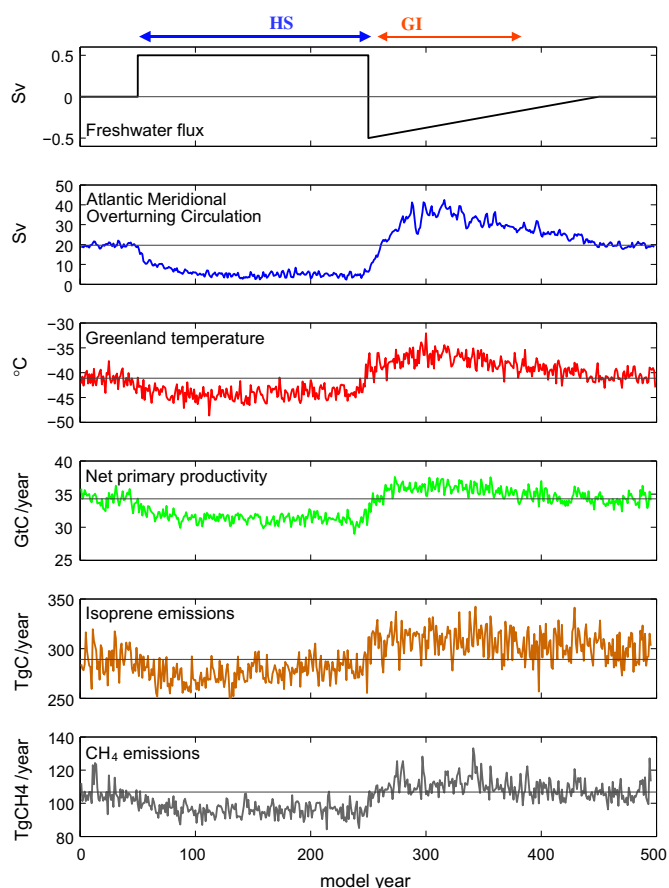
Fig. 4. Freshwater input, and simulated timeseries of Atlantic MOC, Greenland temperature, and global net primary productivity, isoprene emissions and wetland CH$_4$ emissions for the LGM simulation. The GI (interstadial) and HS (stadial) phases of the forcing are identified at the top of the figure.

results from both FAMOUS (used in this study) and its higher resolution parent model HadCM3 which we have not used because it is much more computationally expensive. We note that FAMOUS contains the same model physics as HadCM3, the major differences being the horizontal resolution and the reduced number of vertical levels in the atmosphere (11 versus 19). The HadCM3 simulations use an identical version of the vegetation and wetlands model except that this is run on the higher resolution horizontal grid. The HadCM3 climate simulations have been described previously (Singarayer and Valdes, 2010; Singarayer et al., 2011).

HadCM3 climatology is assessed by Randall et al. (2007) and a comparison with FAMOUS is given by Smith et al. (2008). We find that FAMOUS precipitation errors are broadly similar to HadCM3, but are larger over both the Amazon and south west USA where FAMOUS is drier than HadCM3, and over Central Africa and Australia for which FAMOUS overestimates precipitation.

In Fig. 2 the pre-industrial fluxes for FAMOUS and HadCM3 are compared with the 1984—2005 mean natural wetland flux from the inversion study of Bousquet et al. (2006). The two model outputs show similar patterns of emissions, with almost equal peaks concentrated around the equator. Both models also show significant mid-latitude emissions which begin to decrease Northwards of 60°N. In the inversion, the pattern is broadly similar although emissions are inferred further North and there are relatively less emissions in the latitudes from 20° to 40°N. In this inversion this area is a significant source of rice paddy CH$_4$ emissions which we have not included in the comparison. The model simulates

potential natural wetland emissions and this area is a significant source of natural CH$_4$ emissions in both models.

In Fig. 2 the changes in zonal emissions for the LGM are shown for the two models. This shows that the patterns of change are very similar. There is a pronounced decrease in mid- to high-latitudes of the Northern Hemisphere, which is somewhat offset by a shift in emissions to lower latitudes, as in the PMIP2 simulations (Weber et al., 2010). The tropics show a more even pattern of emissions reductions which appear proportional to the pre-industrial emission rates. Comparison of total global emissions for the pre-industrial and LGM for the two models are shown in Table 1. The reduction during the LGM is 43% in FAMOUS and 32% in HadCM3, suggesting that the FAMOUS climate leads to slightly higher wetland sensitivity to the imposed LGM boundary conditions. This sensitivity is mostly due to changes in the tropical regions (Table 1) which, in HadCM3 show a reduction in the western Amazon basin and an increase to the East, reminiscent of the El-Ñino precipitation pattern (not shown). This is not replicated in FAMOUS, possibly due to the lower resolution, and instead there is a general reduction in emissions throughout the Amazon region.

Fig. 3 compares the seasonal evolution of emissions averaged over the region polewards of 45°N for the two climate models and the Bousquet et al. (2006) model output. The two climate models show almost identical seasonal responses in this region, with a well defined seasonal peak during July. This is replicated in the data but the emissions are generally spread throughout more of the year, with higher winter emissions than in the model, similarly to Ref. Ringeval et al. (2010). Tropical emissions show similar mean annual values and amplitudes of seasonal variability, but the timing shows little agreement between the two models and the inversion data (not shown).

The model data comparison is not ideal, since the model outputs represent potential natural wetland emissions, in the absence of anthropogenic interference and because the modelled time period does not coincide with the data study period. Overall however, the reasonable agreement between the two models and the inversion data, suggests that the model framework can usefully predict wetland emissions (e.g. Valdes et al., 2005; Singarayer et al., 2011), and that the lower resolution of FAMOUS does not significantly degrade the simulation of global CH$_4$ emissions. This gives us confidence to employ this model in other climatic states such as for D-O events.

3.2. Response to freshwater forcing

In the LGM climate simulation with freshwater forcing, the 30-year mean AMOC reduces to almost no overturning and then increases rapidly, leading to a peak of 36.9 Sv which is 17.2 Sv above the non-forced LGM value (Table 2). The timeseries of the maximum of the AMOC streamfunction is shown in Fig. 4. The AMOC off phase is here denoted as analogous to a Heinrich stadial ('HS') whilst the strong overturning behaviour is denoted as analogous to a Greenland Interstadial ('GI'), see Ref. Sanchez-Goñi and Harrison (2010) for more detail of these definitions. Defining the

Table 1
Simulated FAMOUS (this study) and HadCM3 (Singarayer et al., 2011) emissions for the pre-industrial and LGM, and 1984—2005 average natural wetland emissions from Bousquet et al. (2006), in Tg CH$_4$/year. (NH-ex denotes > 45°N).

GCM	Pre-ind.			LGM		
	NH-ex	Tropical	Global	NH-ex	Tropical	Global
Bousquet et al.	53.8	108.0	165.7	—	—	—
FAMOUS	70.0	130.3	193.6	36.5	72.1	108.8
HadCM3	71.5	113.4	185.2	39.8	86.8	126.8

Table 2
30-year mean values for the pre-industrial and four time periods in the transient LGM simulation with freshwater forcing.

Time period	Pre-industrial	LGM	HS	GI	–
Years	–	1–30	201–230	301–330	451–480
AMOC[a] (Sv)	17.5	19.6	4.7	36.8	19.5
Greenland SAT (°C)	−20.4	−41.1	−43.8	−36.5	−40.8
NPP (GtC/year)	56.2	34.3	31.3	36.2	34.0
Isoprene emissions (Tg C/year)	696.8	289.1	281.9	310.1	298.1
CH$_4$ emissions (Tg CH$_4$/year)	193.6	108.8	99.1	114.7	107.5

[a] The maximum of the annual mean overturning streamfunction below 500 m.

different phases of the simulation for comparison with the data is not straightforward. For example, for the overall amplitude of the warming phase of the simulated D-O event, it is unclear as to whether it should be taken as the shift from an initial unperturbed equilibrium state to the transient forced warm state, or from a quasi-transient cold state to transient warm state. In subsequent analyses we compare the magnitudes of both transitions.

The freshwater input results in a significant decrease in the poleward transport of heat by the overturning circulation. During the GI this situation is reversed, and 10-year mean temperatures increase by up to 16 °C in the vicinity of the North Atlantic (Fig. 5), with smaller changes over Greenland of around 5 °C compared to the unperturbed state, see Fig. 4 and Table 2. The signal is abrupt, with Greenland warming of 4 °C occurring within 10 years, and followed by a more gradual rise of a further 5 °C in 50 years. The AMOC increases almost linearly over the same time period, but peaks approximately 10 years earlier than Greenland temperatures. Globally, temperatures gradually return to unperturbed levels as the freshwater forcing is reduced to zero.

The effect of the delivery of a large amount of freshwater to the North Atlantic has been examined previously in so-called 'hosing'

experiments with coupled general circulation models (Vellinga and Wood, 2002; Stouffer et al., 2006). The major feature is a large scale Northern Hemisphere cooling, with a southward shift of the ITCZ and concurrent, strong change in global precipitation patterns. These changes are replicated in the HS part of the climate model experiments presented here with a maximum 10-year mean cooling of 10 °C, although again this signal is smaller over Greenland, see Fig. 5.

The response to invigoration of the AMOC (GI) is not antisymmetric about the unperturbed state, and although the effect on surface temperatures is large, there are relatively modest changes to global precipitation patterns (see Fig. 5), with a weak increase in precipitation in the region of the North Atlantic which is associated with the direct effects of increased temperatures. This result is important for the subsequent analysis of CH$_4$ emission changes and so we compared the climatic response simulated here with results from the CCSM model in which an abrupt strengthening of the AMOC also occurs (Liu et al., 2009). In CCSM, precipitation behaves in a very similar manner as in FAMOUS (Z. Liu and F. He, personal communication) and we therefore believe that the broad patterns of change simulated here are robust to model uncertainties. However, we note that there are differences between climatic responses to freshwater input in different models (Stouffer et al., 2006), and recent studies have also shown sensitivity to other boundary conditions (glacial or interglacial) and the precise location of freshwater input (e.g. Smith and Gregory, 2009; Swingedouw et al., 2009; Kageyama et al., 2010).

The ICTZ shift in the HS period results from a modification of the latitudinal temperature gradients in the tropical Atlantic, itself partially caused by an increased gyre transport of cold (and fresh) water southwards (which would help to aid eventual recovery of the AMOC in the absence of continued freshwater forcing). However, when the AMOC is strengthened through the imposed salinification of the surface water, it transports the excess dense water to depth. Thus a large tropical thermal contrast cannot
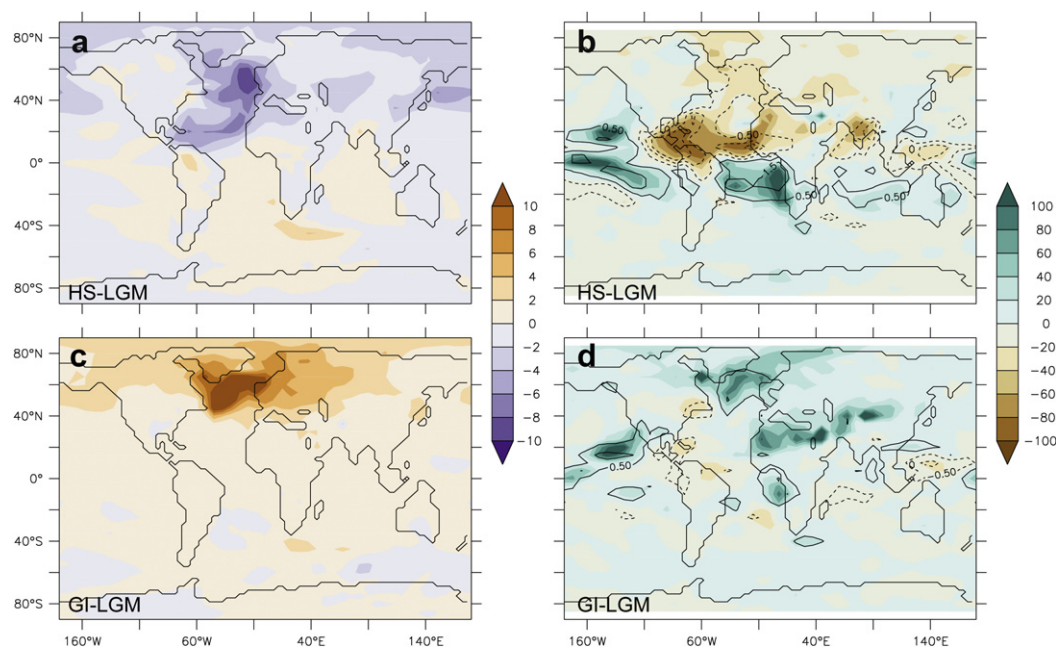
Fig. 5. Climatic anomalies due to freshwater forcing. (a,c) Surface air temperature (°C) and (b,d) surface precipitation anomalies relative to the unperturbed LGM state (colours % and contours in mm/day with levels at −1.5,−0.5,0.5,1.5). Top panels show the anomaly during the simulated Heinrich stadial and the bottom figures show the anomaly during the Greenland interstadial, both for the transient LGM simulation. Peak warming during GI in the North Atlantic is 16.9 °C and maximum cooling during the HS is 9.8 °C. The total temperature range in the North Atlantic is 21.7 °C as the regions of warming and cooling do not coincide. (For interpretation of the references to colour in this figure legend, the reader is referred to the web version of this article.)

develop, and the ITCZ remains relatively unperturbed from its LGM position. This contrast between HS and GI tropical precipitation signals appears to be supported by speleothem and vegetation paleo-records from the tropical sites (Wang et al., 2004; Harrison and Sanchez-Goñi, 2010; Hessler et al., 2010) which show stronger evidence for precipitation change during HS events as compared with more frequent GI events.

Modelled global vegetation responds strongly to climate changes associated with the forced AMOC variations. The global net primary productivity is reduced by 3 GtC/year and increases by 1.9 GtC/year in response to AMOC perturbations (Fig. 4 and Table 2). The larger HS decrease reflects significant NPP reductions around the equator, whilst during the GI stage, these reductions persist, but are countered by a small increase over most of the Northern Hemisphere. Isoprene emissions respond with a small reduction during the HS but a more significant increase during the GI phase.

The resultant emissions of CH_4 are also shown in Fig. 4 and spatially in Fig. 6. The peak anomaly (i.e. minus the unforced LGM state) is around 25 Tg CH_4/year, but this is relatively short lived and the 30-year mean anomaly is only around 10 Tg CH_4/year. This corresponds to small increases in Northern Eurasia, but with relatively little change in the tropical regions where the majority of emissions occur (Fig. 6 d). The emissions are reduced significantly during the hosing stage (Fig. 6 a) and the southward movement of the ITCZ can also be seen in the emission changes. The spatial change in emissions between the hosing (HS) and warming phase (GI) shows a general increase in Northern hemisphere emissions (Fig. 6 c).

The difference between the warm and equilibrium LGM emissions (GI-LGM) equates to around 10% of the glacial-interglacial (G-IG) difference as simulated with the same model framework (as shown in Table 2). None of the D-O events in the Greenland record are this small, possibly with the exception of event number 2 (Fig. 1). The modelled increase in emissions therefore appears to significantly underestimate the magnitude of the majority of ice-core reconstructed D-O CH_4 fluctuations, which attain a significant fraction of the glacial-interglacial concentration amplitude (i e. 150–200 ppbv), for example, see D-O events 1,5–8, 12, 15–17. If however, the D-O warming is taken as the perturbation over the total simulated amplitude of AMOC change (i.e. from HS to GI) then the CH_4 emissions change is approximately 20% of the G-IG amplitude, and this change is closer but still not fully reconcilable with some of the smaller D-O events. For example the concentration change during events 3,10,11,19 and 20 is around 100 ppbv, or 30% of G-IG concentration change. Since these simulation results are only directly relevant for comparison with the time period around the LGM at 21 kyr, we next examine the extent to which the background climatic state (ice sheet distribution, atmospheric greenhouse gas levels and orbital insolation) might affect the CH_4 emission response to freshwater.

3.3. Sensitivity to background climatic state

A key feature of the ice-core record of CH_4 is the variability in the amplitude of the abrupt increases during D-O events. This is illustrated by Greenland temperature (Masson-Delmotte et al., 2005) and atmospheric CH_4 (Blunier and Brook, 2001; Flückiger et al., 2004; Huber et al., 2006) for the period from 80 to 10 kyr before present (Fig. 1). There is no clear relationship between the magnitude of the rise of temperature and of CH_4. For example, the CH_4 jumps gradually diminish in amplitude during the course of D-O events 8 to 3, whereas the Greenland temperature rises are relatively constant (see Fig. 1). Also, D-O events 19 and 20 display very large temperature changes but relatively modest CH_4 excursions, suggesting a non-linear relationship between high-latitude temperature and global CH_4. The D-O CH_4 signal does appear to be modulated at an orbital time-scale (e.g. Flückiger et al., 2004), suggesting the possible importance of orbital insolation, global ice volume or greenhouse gas levels, all of which varied with similar periodicities. We therefore explored the influence of the background state on the magnitude of the simulated CH_4 emissions in a series of further simulations testing for the influence of the land ice sheet extent, orbital insolation and atmospheric CO_2 concentrations.
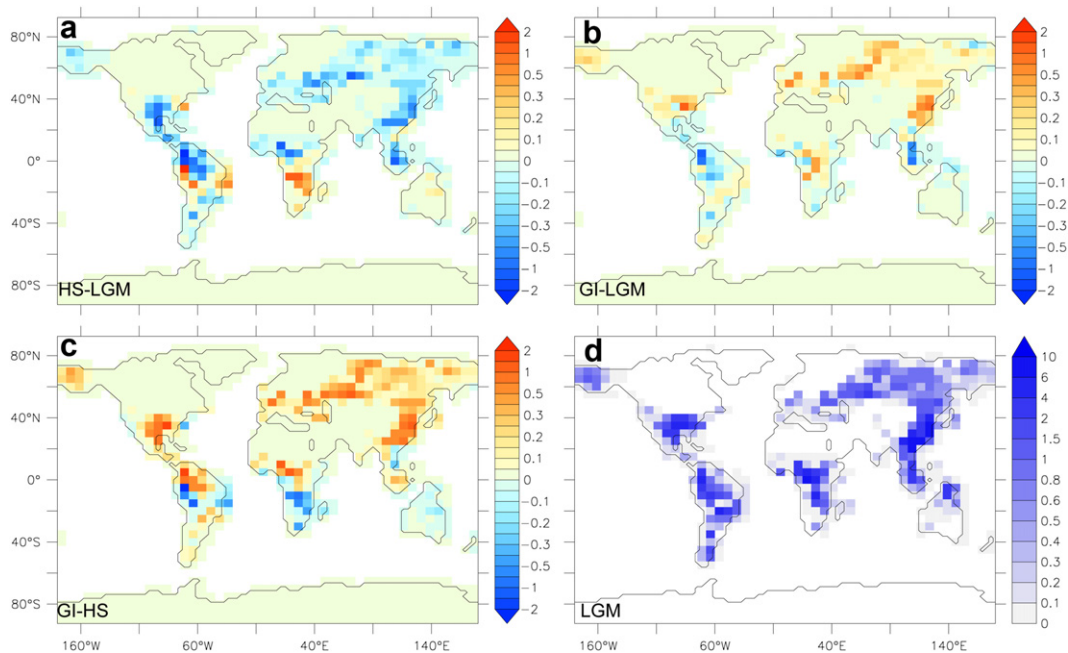
Fig. 6. CH_4 emission anomalies due to freshwater forcing, HS is stadial or hosing stage, GI is the warm phase and LGM denotes the equilibrium non-forced LGM conditions. Units are gCH_4 m^{-2} year^{-1}. The emissions have been corrected with the fractional land sea mask.

The simulations are based on either the LGM simulation or a LGM simulation configured with pre-industrial land ice. The effects of 84 kyr orbital insolation and pre-industrial CO_2 (=280 ppmv) have also been tested. 84 kyr orbital insolation was chosen because of the particularly large D-O CH_4 jump in the record at this time (Grachev et al., 2007), and because it represents a precessional minimum (i.e. Northern Hemisphere summer insolation is enhanced relative to the modern, and the summer monsoon systems are intensified with potential impacts for wetlands and CH_4 production).

Huber et al. (2006) compared D-O events 9–17 in terms of rates and magnitudes of change. Their work suggested an increasing ratio of CH_4 relative to Greenland temperature especially for events 15–17 which occurred between 55.8 and 59.2 kyr bp (Wolff et al., 2010). A similar comparison is shown for the 5 sensitivity simulations and the predicted [CH_4] in Table 3. The results show that the temperature changes in Greenland are relatively constant, at about 6–8 °C, except in the case of the LGM + P.I. ice + 84 kyr orbitals, for which ΔT is only 4.6 °C. These values are less than recorded in ice-core data which generally show amplitudes of 8–16 °C. This temperature underestimate for Greenland may be related to deficiencies in the simulation of the North Atlantic atmospheric circulation in FAMOUS.

The changes in simulated CH_4 emissions from these simulations are shown together with the values from the original LGM simulation in Fig. 7. The variability in the magnitude of the HS signal is large, with the most significant decrease seen in the 84 kyr simulation with pre-industrial ice. This can be attributed to the greater effect from the change in the ICTZ under these conditions, when the low latitude hydrological cycle is intensified by stronger land sea thermal contrasts.

The simulation with pre-industrial CO_2 shows the largest increase in CH_4 emissions, but this is entirely due to the effects of CO_2 fertilization (repeating the simulation with an LGM CO_2 specified in the vegetation model brings the emissions down to the similar values as in the other simulations). However, no scenario leads to a significant increase in the modelled CH_4 during the GI. Instead, significant variability is manifest only during the HS phases when the modelled ITCZ is significantly perturbed. This suggests a dominant role for lower latitude regions in the precessional variations of the magnitude of D-O events in the CH_4 record, and also potentially in long-term atmospheric CH_4 concentration variations. However, as the model used here does not explicitly resolve permafrost thermodynamics that may be important for simulating high-latitude emissions, we cannot rule out a role for these regions also.

The maximum simulated emissions increase is 20% of the G-IG range for the LGM simulation and this is enhanced to around 35% (G-IG range) for the 84 kyr orbital plus pre-industrial ice. If only the orbital insolation is modified, the amplitude is slightly smaller (30%). These emissions changes appear consistent with the smaller
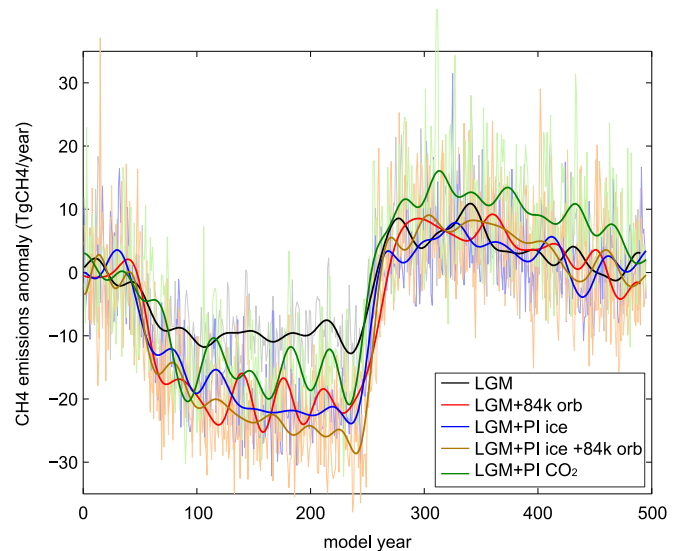

Fig. 7. Annual CH_4 emission changes for differing background states. LGM, LGM with 84k orbital insolation, LGM with pre-industrial land ice and sea level, LGM greenhouse gases with 84k orbital insolation and pre-industrial land ice and sea level and LGM but with pre-industrial CO_2. LGM denotes Peltier (2004) ice sheets and sea level, 21 kyr greenhouse gas levels and 21 kyr orbital insolation. Land cover properties in the climate model are set to the pre-industrial distribution except where land ice or sea level changes overprint these.

D-O events when the total range of the simulated perturbation is considered, i.e. from AMOC off to a forced AMOC strong state (GI-HS). If the change between the non-forced LGM and the GI state is used, then again the increase in emissions in all of the simulations considered is likely too small compared with all of the D-O events. Given that we have used end-member points for these idealized experiments (i.e. fully interglacial ice sheets or CO_2, and a precessional minimum) it is likely that more realistic boundary condition changes relating to the last glacial cycle will produce less variability than simulated here. For example, the global distribution of land ice during Marine Isotope Stage 3 was probably around half the mass of the LGM ice sheet and CO_2 levels during this time period were similarly intermediate between glacial (180 ppmv) and interglacial values (280 ppmv).

3.4. Concentration prediction and influences on lifetime

In order to facilitate a more detailed comparison between our model outputs and the ice-core record we have attempt to calculate the likely impact from the simulated emission changes on atmospheric CH_4 concentrations. We use the simulated emissions of CH_4 and optionally VOCs in a simple budget approach which relies on the well-known equation (e.g. Etheridge et al., 1998; Lassey et al., 2007):

$$\frac{dB}{dt} = S - \frac{B}{L}, \tag{1}$$

where B is the atmospheric CH_4 burden (in Tg), S are global CH_4 emissions (Tg CH_4 year^{-1}) and L is the atmospheric CH_4 lifetime (in years). In the first instance we assume that L is a constant ($L_0 = 8.6$ years) and so variability is only introduced through changing emissions. However, a number of factors influence the residence time of CH_4 in the atmosphere through modification of the strength of the principal sink (reaction with OH). These include temperature, and humidity, as well as the concentration of CH_4 itself and levels of VOCs such as isoprene.

Table 3
Greenland temperature, T (°C) and atmospheric CH_4 concentration (ppbv) changes for the different sensitivity simulations, where eq refers to the initial stage of the simulation for which the freshwater forcing is zero. All values are calculated from 20 year means.

Simulation	ΔT		Δ [CH_4]		Δ [CH_4]/ΔT
	GI-eq	GI-HS	GI-eq	GI-HS	GI-HS/GI-HS
LGM	4.9	7.7	11	48	6.3
LGM + 84k orb	3.5	6.5	28	96	14.8
LGM + P.I. ice	4.7	6.0	18	93	15.5
LGM + P.I. ice + 84k orb	4.5	4.6	23	111	24.1
LGM + P.I. CO_2	4.6	7.6	32	53	7.0

Sensitivity studies with STOCHEM (Valdes et al., 2005) and p-TOMCAT (Levine et al., 2011) both suggest that the self-feedback of CH_4 for the glacial is of the order of 10%. Valdes et al. (2005) found that an emissions increase by a factor of 1.26 lead to a 1.37 factor increase in concentration, whilst Levine et al. (2011) conducted two sensitivity tests for CH_4 emissions and found increases in emissions by factors of 1.2 and 1.82 lead to concentration increases by factors of 1.28 and 2.08 respectively. We therefore multiply the concentration changes derived here by 10%, as an approximation of this self-feedback effect. The effects of changes in temperature and humidity on the lifetime could counter or reverse the sign of the total lifetime feedback from the combined effects of climate and CH_4, but we have not attempted to include this effect in our calculations.

Previous studies have suggested that VOC emissions are important for the glacial to interglacial change in CH_4 levels (Valdes et al., 2005; Kaplan et al., 2006). In order to explore whether VOCs may also be important in abrupt events, we also examine a linear dependency of atmospheric CH_4 lifetime on the modelled time-dependent isoprene emissions. For this, the lifetime is taken as:

$$L(t) = L_0 + 0.0036 \times (I(t) - 594.4), \quad (2)$$

where $I(t)$ are annual isoprene emissions (Tg C/year) and the remaining values are derived from sensitivity simulations with the 3D atmospheric chemistry models STOCHEM and p-TOMCAT (Valdes et al., 2005; Levine et al., 2011). In calculating these values, we assume that other VOC emissions also change in a similar proportion to isoprene as simulated by Valdes et al. (2005). Isoprene emissions are also corrected for the atmospheric CO_2 concentration using the relation of Possell et al. (2005), normalized to unity for $CO_2 = 366$ ppmv. This increases isoprene emissions under low ambient CO_2 in accordance with experimental results (Possell et al., 2005). As the CO_2 concentration is constant it has no influence on the time-dependent behaviour of the model.

It should be noted that predictive modelling of isoprene emissions is subject to a reasonable level of uncertainty since many of the underlying controls on emissions are not well understood (Monson et al., 2007; Arneth et al., 2008), and furthermore the link between forest level and atmospheric chemistry appears to be more complex than previously assumed (Lelieveld et al., 2008). The results derived using equation (2) should therefore be viewed with some caution.

3.5. Emissions only concentration predictions

Fig. 8 shows the resulting concentrations calculated with a constant lifetime L_0 and with a variable value calculated for each model year as above, $L(t)$. The concentration changes are largest in both cases for the simulation with pre-industrial ice and modified (84 kyr) orbital insolation. In almost all of the simulations, the GI change relative to the unforced climate phase is very small and of the order of 30 ppbv. The total concentration change (GI-HS) is larger, and is of the order of 70 ppbv for the LGM and LGM + pre-industrial CO_2. As in Fig. 7 the other simulations show stronger responses during the HS phase, and for these the total [CH_4] change ranges up to 110 ppbv.

The ratio of CH_4 change to Greenland temperature change could provide a useful diagnostic of the model sensitivity and is shown for the 5 sensitivity simulations in Table 3. The ratio varies from around 6 (ppbv/°C) in the LGM simulation up to 24 for the LGM + 84 kyr orbital and P.I. ice. Huber et al. (2006) calculated this range based on Greenland ice-core data, with values ranging from 7 to 16 over the course of D-O events 9–17. The simulations are therefore approximately consistent with the data-based values, but
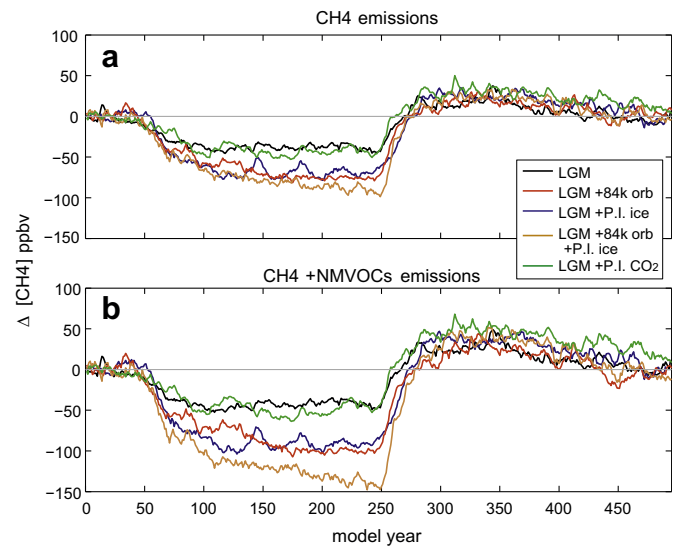
Fig. 8. Calculated atmospheric CH_4 concentration changes resulting from (a) simulated CH_4 emissions and (b) additionally including an estimate of the influence of isoprene on the lifetime of atmospheric CH_4. All timeseries are amplified by 10% to account for the self-feedback of CH4.

the simulations underestimate changes in both Greenland temperature and CH_4. The higher value of this ratio inferred from the ice-core data during D-O events 15–17 compared to later events (D-O 9–12) coincides with an increase in orbital precession, whereas the sea level difference between the two time periods was quite modest. The sensitivity of the model to orbital insolation therefore appears consistent with this trend in the data, but more quantitative comparisons would require further simulations with more realistic boundary conditions.

In our results the rapidity of the CH_4 change is similar to the 100 year time-scale of change observed in the ice-core data. For example, in experiments with constant lifetime (shown in Fig. 8), CH_4 takes about a century to increase from the minimum to maximum value, with an initial rapid increase followed by a slower increase of smaller amplitude which corresponds to the GI warming phase. The issue of the time-scale of change is difficult to address however, given that the results are highly dependent on the freshwater forcing employed.

3.6. Potential influence of VOCs

The influence of the isoprene parameterisation is shown in Fig. 8. It is stronger and shows more variability between the simulations during the HS. For example, the influence of isoprene can be clearly seen in the simulation with 84 kyr orbital insolation and pre-industrial ice which is nearly 50 ppbv larger change during the HS but with a nearly identical signal during the GI as in the other simulations. Since isoprene is primarily emitted in the tropics, the influence of the background state is different from that on CH_4 emissions as shown in Fig. 4. Despite a large difference in the modelled VOC emissions between the LGM and the LGM + pre-industrial CO_2 experiments, the correction for sub-ambient CO_2 means that the effect on the CH_4 lifetime is approximately similar between these two simulations, as shown in Fig. 8.

Including the VOC effect, the change in CH_4 concentrations predicted here for the warm phase relative to the non-forced state is always too small in comparison with the D-O record. However, if the total amplitude of simulation is considered then the comparison becomes more favourable, especially if the effects of isoprene on atmospheric chemistry are used. In this case the maximum
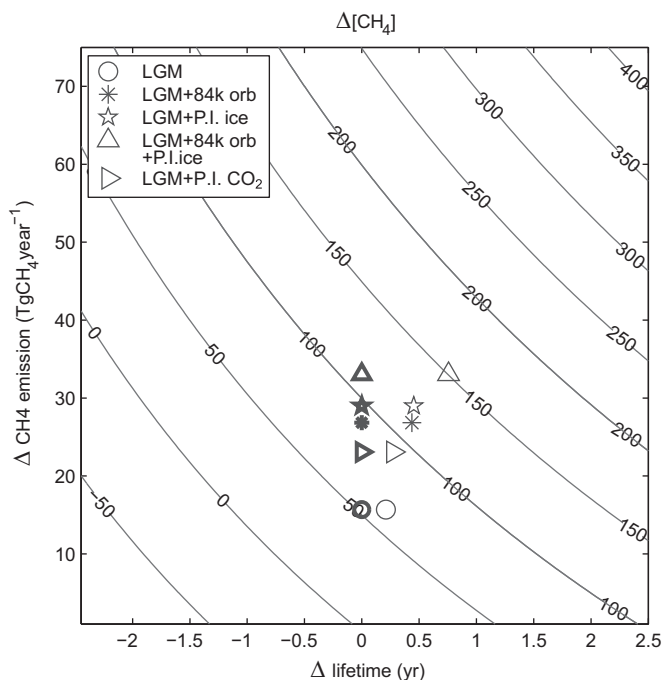
Fig. 9. Contour plot of [CH_4] change as a function of atmospheric lifetime and emissions changes, including a 10% CH_4 self-feedback factor. The envelope of 100–200 ppbv encompasses the approximate range of the majority of D-O events. The results from the FAMOUS + SDGVM simulations are shown (bold denotes constant lifetime, the others show the calculated lifetime change due to variations in VOC emission rates.).

amplitude of change varies between around 80 ppbv for the LGM case, 110 ppbv if the orbitals or ice sheet are changed, and 160 ppbv for the LGM + 84 kyr orbital + pre-industrial ice.

3.7. Reconciling the model simulations with the ice-core record

In order to be able to reconcile our model results with the ice-core data we therefore require an AMOC perturbation from essentially zero overturning to approximately double the non-forced value (i.e. 35–40 Sv), coupled with a significant atmospheric chemistry effect from changes in global VOC emissions. Only then do we simulate changes of the same order of magnitude as majority of the D-O events observed in the ice-core record. We note that the total temperature change simulated over the North Atlantic for the full amplitude of AMOC change (22 °C) exceeds that reconstructed from Greenland ice-core data (8–16 °C), see Fig. 5. A background climate with pre-industrial ice volume and with a low value of orbital precession amplifies the change, as in observations. However, for such climatic states, the ice-core record suggests D-O events of up to 200 ppbv, for example during the Last Interglacial, D-O event 21 (Grachev et al., 2007) and during the Bølling-Allerød warming (D-O 1), indicating that our model is underestimating the largest events even with idealized (interglacial) boundary conditions.

In Fig. 9 a simplified calculation of the theoretical change in [CH_4] resulting from different combinations of emissions or CH_4 lifetime changes is shown. This calculation uses equation (1) and assumes equilibrium states for the HS and GI as well as a CH_4 self-feedback strength of 10%, described earlier. The approximate window of observed D-O event magnitudes is 100–200 ppbv. It can be seen that for the larger events the emissions must increase significantly by around 60 Tg CH_4/year, unless there is a simultaneous, large increase in the lifetime. For a 2 year increase in the lifetime, the emissions must still increase by 30 Tg CH_4/year in order to produce a 200 ppbv growth in concentration. The

equilibrium changes in [CH_4] as calculated from the model output using 30-year means of GI minus HS are shown for the 5 sensitivity simulations. The lifetime changes are calculated from the times-eries of L calculated with equation (2). This comparison highlights that neglecting the influence of VOCs, no simulation can match the larger D-O events of 200 ppbv. Even considering the VOC effect, all but one of the simulations lies in the region 50–125 ppbv which is significantly lower than the observed range (100–200 ppbv) of abrupt CH_4 increases during D-O events.

4. Discussion and conclusions

The ice-core records of CH_4 (as well as dust and N_2O) provide valuable constraints for improved understanding of D-O variability. We have attempted to exploit this dataset in a comprehensive Earth System modelling framework. We have shown that AMOC changes are insufficient to reproduce most of the large, abrupt rises in CH_4 in the ice-core record, despite using fairly large freshwater forcings in our simulations. This underestimation of CH_4 change could result from four different factors: (i) the model setup is too insensitive to the appropriate climate changes, (ii) the forcing scenario employed is incomplete, (iii) our scenario of climate forcing (i.e. freshwater forcing leading to AMOC change) is incorrect, or (iv) our assumptions regarding the change in CH_4 lifetime are in error. Further experiments with different models are required in order to differentiate between these possibilities. Interestingly, when we repeated the LGM simulation with double the freshwater forcing rate (i.e. ±1.0 Sv rather than ±0.5 Sv), the results appear very similar, suggesting that there is a threshold over which the AMOC-climate response remains broadly similar.

Changes to the background climatic state modulate both the equilibrium level of emissions as well as the magnitude of the abrupt change of CH_4 emission changes during the stadial phases of these simulations. The background state also has a strong influence on the magnitude of simulated VOC emissions and this shows a different dependence to CH_4, because for example, isoprene, is emitted over different regions than CH_4. The results suggest that changing background climatic state (e.g. global ice volume or orbital precession) has the potential to produce variable magnitude of CH_4 changes during D-O events as in the observations. The absence of strong D-O events during the last glacial maximum however, suggests that model boundary conditions for the other times in the glacial period might be usefully investigated, particularly Marine Isotope Stage 3 because there are a series of stronger and weaker events over this time period.

Our results suggest that changes in VOC emissions could significantly modify the atmospheric CH_4 response during D-O events, but recent studies (e.g. Monson et al., 2007; Arneth et al., 2008) suggest that more research is required to determine the dominant controls of isoprene emission. The sinks of CH_4 are also influenced by temperature and humidity. Valdes et al. (2005) showed that changes in temperature from LGM to pre-industrial could only account for 10% of the total CH_4 variation. Since the temperature changes during a D-O cycle are smaller than this, we do not believe that this would significantly modify our conclusions. Recently Prather and Hsu (2010) demonstrated a coupling between atmospheric N_2O and CH_4 through stratospheric chemistry, which suggests that an increase in N_2O leads to a concomitant decrease in CH_4 levels. Since both trace gases rose abruptly during most D-O events (Flückiger et al., 2004), this implies larger CH_4 emissions are required in order to produce the same CH_4 concentration change as would occur in the absence of any N_2O increase.

A compilation of charcoal records for the glacial period shows some co-variability during D-O events (Daniau et al., 2010) suggesting that biomass burning could contribute to the D-O CH_4 signal.

However, natural fire related emissions currently contribute less than 5% the CH_4 emissions from wetlands (Denman et al., 2007) suggesting that they are unlikely to significantly affect the atmospheric concentration. Modelling of biomass burning and CH_4 is an active area of research and, to our knowledge, quantitative estimates for past regimes such as D-O events have yet to be produced. Biomass burning also has an influence on the atmospheric lifetime of CH_4 through chemical reactions of CO and NO_x. Sensitivity tests with STOCHEM (Valdes et al., 2005) suggest that the NO_x emission changes are unlikely to play a large role in the observed CH_4 changes, but the role of changes in CO requires further study in this context.

The sensitivity of the model climate to freshwater input is an important factor determining responses in the current work. Compared to other AO-GCMs HadCM3 (the parent model of FAMOUS) displays less than the model average temperature change in response to 0.1 Sv forcing (Stouffer et al., 2006). Our analysis of the THCMIP data shows that for a 1.0 Sv forcing, HadCM3 has a similar magnitude of response to the AOGCM ensemble mean (Stouffer et al., 2006), although the area of cooling exceeding 10 °C is smaller and is confined to the Barents Sea region. We compared HadCM3 with FAMOUS under LGM conditions and after a 1.0 Sv by 100 year forcing and found broadly similar patterns and magnitudes of temperature and precipitation change in the two models. The temperature change over Greenland was markedly smaller in FAMOUS than in HadCM3 however, and this may reflect a tendency towards overly zonal atmospheric flow in this version of FAMOUS. Furthermore, summer (JJA) precipitation and temperature increases in FAMOUS over the Amazon are smaller than in HadCM3, although the winter (DJF) responses are comparable in the two models.

Our simulation results point towards an AMOC based explanation for some of the variability between D-O events, but other climatic mechanisms may be required in order to reconcile the model with the large CH_4 changes recorded in the ice-core data. This would also call into question the underlying climatic drivers of D-O variability. Our conclusion would be especially robust if the model over-predicts changes in VOCs, or if their influence on the CH_4 lifetime is significantly weaker than we have assumed (e.g. Lelieveld et al., 2008). Wunsch (2006) suggested that future studies of D-O climate changes should consider the interaction of the wind field with ice-age topography rather than the AMOC, as examined here and in most previous work. Seager and Battisti (2007) also discuss alternative mechanisms of D-O climate change and suggest a role for the tropics via interaction with the Northern Hemisphere jet streams. These may also be promising areas for investigating D-O CH_4 changes. One physical process worthy of consideration in this context is the El Niño-Southern Oscillation (ENSO), which is not realistically represented in the climate simulations presented here (due to the lower horizontal model resolution). ENSO exerts a strong influence on inter-annual CH_4 concentrations in the contemporary Earth System and a shift to more frequent La Niña conditions during a D-O event could help to explain the magnitude of abrupt CH_4 increase. Future research could consider the link between the Atlantic MOC and ENSO (e.g. Dong et al., 2006; Timmermann et al., 2007) as well as examining how independent models respond to similar forcings and climatic states as tested here.

Acknowledgements

References

Arneth, A., Monson, R., Schurgers, G., Niinemets, U., Palmer, P., 2008. Why are estimates of global terrestrial isoprene emissions so similar (and why is this not so for monoterpenes)? Atmos. Chem. Phys. 8, 4605–4620.

Beerling, D.J., Woodward, F.I., 2001. Vegetation and the Terrestrial Carbon Cycle: Modelling the First 400 Million Years. Cambridge University Press, Cambridge.

Blunier, T., Brook, E., 2001. Timing of millennial-scale climate change in Antarctica and Greenland during the last glacial period. Science 291, 109–112.

Bock, M., Schmitt, J., Moller, L., Spahni, R., Blunier, T., Fischer, H., 2010. Hydrogen isotopes preclude marine hydrate CH_4 emissions at the onset of Dansgaard-Oeschger events. Science 328, 1686–1689.

Bousquet, P., Ciais, P., Miller, J., Dlugokencky, E., H., D., Prigent, C., Van der Werf, G., Peyling, P., Brunke, E.-G., Carouge, C., Langenfelds, R., Lathiere, J., Papa, F., Famonet, M., Schmidt, M., Steele, L., Tyler, S., White, J., 2006. Contribution of anthropogenic and natural sources to atmospheric methane variability. Nature 443, 439–443.

Braconnot, P., Otto-Bliesner, B., Harrison, S., Joussaume, S., Peterchmitt, J.-Y., Abe-Ouchi, A., Crucifix, M., Driesschaert, E., Fichefet, T., Hewitt, C., Kageyama, M., Kitoh, A., Laine, A., Loutre, M.-F., Marti, O., Merkel, U., Ramstein, G., Valdes, P., Weber, S., Yu, Y., Zhao, Y., 2007. Results of PMIP2 coupled simulations of the Mid-Holocene and Last Glacial Maximum part 1: experiments and large-scale features. Clim. Past 3, 261–277.

Broecker, W.S., Peteet, D.M., Rind, D., 1985. Does the ocean-atmosphere system have more than one stable mode of operation? Nature 315, 21–26.

Cao, M., Marshall, S., Gregson, K., 1996. Global carbon exchange and methane emissions from natural wetlands: application of a process-based model. J. Geophys. Res. 101 (D9), 14399–14414.

Cattle, H., Crossley, J., 1995. Modelling Arctic climate-change. Philos. Trans. R. Soc. A 352, 201–213.

Chappelaz, J., Blunier, T., Raynaud, D., Barnola, J., Schwander, J., Stauffer, B., 1993. Synchronous changes in atmospheric CH_4 and Greenland climate between 40 and 8 kyr BP. Nature 366, 443–445.

Clark, P., Pisias, N., Stocker, T., Weaver, A., 2002. The role of the thermohaline circulation in abrupt climate change. Nature 415, 863–869.

Cox, P.M., Betts, R.A., Bunton, C.B., Essery, R.L.H., Rowntree, P.R., Smith, J., 1999. The impact of new land surface physics on the GCM simulation of climate and climate sensitivity. Clim. Dyn. 15 (3), 183–203.

Dällenbach, A., Blunier, T., Flückiger, J., Stauffer, B., Chappellaz, J., Raynaud, D., 2000. Changes in the atmospheric CH_4 gradient between Greenland and Antarctica during the Last Glacial and the transition to the Holocene. Geophys. Res. Lett. 27 (7), 1005–1008.

Daniau, A.-L., Harrison, S., Bartlein, P., 2010. Fire regimes during the Last Glacial. Quaternary Sci. Rev. 29, 2918–2930.

Dansgaard, W., Johnsen, S., Clausen, H., Dahl-Jensen, D., Gundestrup, N., Hammer, C., Hvidberg, C., Steffensen, J., Sveinbjornsdottir, A., Jouzel, J., Bond, G., 1993. Evidence for general instability of past climate from a 250 kyr ice-core record. Nature 364, 218–220.

Denman, K., Brasseur, G., Chidthaisong, A., Ciais, P., Cox, P., Dickinson, R., Hauglustaine, D., Heinze, C., Holland, E., Jacob, D., Lohmann, U., Ramachandran, S., da Silva Dias, P., Wofsy, S., Zhang, X., 2007. Couplings between changes in the climate system and biogeochemistry. In: Solomon, S., Qin, D., Manning, M., Chen, Z., Marquis, M., Averyt, K.B., Tignor, M., Miller, H.L (Eds.), Climate Change 2007: The Physical Science Basis: Contribution of Working Group I to the Fourth Assessment Report of the Intergovernmental Panel on Climate Change. C.U.P, Cambridge, U.K. and New York, U.S.A.

Dong, B., Sutton, R.T., Scaife, A.A., 2006. Multidecadal modulation of El Nino-Southern Oscillation (ENSO) variance by Atlantic Ocean sea surface temperatures. Geophys. Res. Lett. 33 L08705.

Etheridge, D.M., Steele, L., Francey, R., Langenfelds, R., 1998. Atmospheric methane between 1000 A.D. and present: evidence of anthropogenic emissions and climatic variability. J. Geophys. Res. 103 (D13), 15,979–15,993.

Fischer, H., Behrens, M., Bock, M., Richter, U., Schmitt, J., Loulergue, L., Chappellaz, J., Spahni, R., Blunier, T., Leuenberger, M., Stocker, T.F., 2008. Changing boreal methane sources and constant biomass burning during the last termination. Nature 452, 864–867.

Flückiger, J., Blunier, T., Stauffer, B., Chappellaz, J., Spahni, R., Kawamura, K., Schwander, J., Stocker, T.F., Dahl-Jensen, D., 2004. N_2O and CH_4 variations during the last glacial epoch: insight into global processes. Glob. Biogeochem. Cycles 18 (GB1020).

Forster, P., Ramaswamy, V., Artaxo, P., Berntsen, T., Betts, R., Fahey, D., Haywood, J., Lean, J., Lowe, D., Myhre, G., Nganga, J., Prinn, R., Raga, G., Schulz, M., Van Dorland, R., 2007. Changes in atmospheric constituents and in radiative forcing. In: Solomon, S., Qin, D., Manning, M., Chen, Z., Marquis, M., Averyt, K.B., Tignor, M., Miller, H.L. (Eds.), Climate Change 2007: The Physical Science Basis: Contribution of Working Group I to the Fourth Assessment Report of the Intergovernmental Panel on Climate Change. C.U.P, Cambridge, U.K. and New York, U.S.A.

Ganopolski, A., Rahmstorf, S., 2001. Rapid changes of glacial climate simulated in a coupled climate model. Nature 409, 153–155.

Gordon, C., Cooper, C., Senior, C.A., Banks, H., Gregory, J.M., Johns, T.C., Mitchell, J.F.B., Wood, R.A., 2000. The simulation of sst, sea ice extents and ocean heat transports in a version of the Hadley Centre coupled model without flux adjustments. Clim. Dyn. 16 (2–3), 147–168.

Grachev, A., Brook, E., Severinghaus, J., 2007. Abrupt changes in atmospheric methane at the MIS 5b–5a transition. Geophys. Res. Lett. 34 (L20703).

Guenther, A., Hewitt, C., Erickson, D., Fall, R., Geron, C., Graedel, T., Harley, P., Klinger, L., Lerdau, M., McKay, W., Pierce, T., Scholes, B., Steinbrecher, R., Tallamraju, R., Taylor, J., Zimmerman, P., 1995. A global model of natural volatile organic compound emissions. J. Geophys. Res. 100 (D5), 8873–8892.

Harrison, S., Sanchez-Goñi, M., 2010. Global patterns of vegetation response to millennial-scale variability and rapid climate change during the last glacial period. Quaternary Sci. Rev. 29 (21–22), 2957–2980.

Hessler, I., Dupont, L., Bonnefille, R., Behling, H., Gonzalez, C., Helmens, K.F., Hooghiemstra, H., Lebamba, J., Ledru, M.-P., Lezine, A.-M., Malye, J., Marret, F., Vincens, A., 2010. Millennial-scale changes in vegetation records from tropical Africa and South America during the last glacial. Quarternary Sci. Rev. 29 (21–22), 2882–2899.

Huber, C., Leuenberger, M., Spahni, R., Flückiger, J., Schwander, J., Stocker, T., Johnsen, S., Landais, A., Jouzel, J., 2006. Isotope calibrated Greenland temperature record over Marine Isotope Stage 3 and its relation to CH_4. Earth Planet. Sci. Lett. 243, 504–519.

Jones, C., Gregory, J., Thorpe, R., Cox, P., Murphy, J., Sexton, D., Valdes, P., 2005. Systematic optimisation and climate simulation of FAMOUS, a fast version of HadCM3. Clim. Dyn. 25, 189–204.

Kageyama, M., Paul, A., Roche, D., van Meerbeeck, C., 2010. Modelling glacial climatic millennial-scale variability related to changes in the Atlantic meridional overturning circulation: a review. Quaternary Sci. Rev. 29 (21–22), 2931–2956.

Kaplan, J., 2002. Wetlands at the Last Glacial Maximum: distribution and methane emissions. Geophys. Res. Lett. 29 (6, 1079).

Kaplan, J., Folberth, G., Hauglustaine, D., 2006. Role of methane and biogenic volatile organic compound sources in the Lateglacial and Holocene fluctuations of atmospheric methane concentrations. Glob. Biogeochem. Cycles 20 GB2016.

Lassey, K., Etheridge, D., Lowe, D., Smith, A., Ferretti, D., 2007. Centennial evolution of the atmospheric methane budget: what do the carbon isotopes tell us? Atmos. Chem. Phys. 7, 2119–2139.

Lelieveld, J., Butler, T., Crowley, J., Dillon, T., Fischer, H., Ganzeveld, L., Harder, H., Lawrence, M., Martinez, M., Taraborrelli, D., Williams, J., 2008. Atmospheric oxidation capacity sustained by a tropical forest. Nature 452, 737–740.

Levine, J., Wolff, E., Jones, A., Hutterli, M., Wild, O., Carver, G., Pyle, J., 2011. In search of an ice core signal to differentiate between source-driven and sink-driven changes in atmospheric methane. J. Geophys. Res. 116 (D05305).

Liu, Z., Otto-Bleisner, B., H., F., Brady, E., Tomas, R., Clark, P., Carlson, A., Lynch-Steiglitz, J., Curry, W., Brook, E., Erickson, D., Jacob, R., Kutzbach, J., Cheng, J., 2009. Transient simulation of Last Deglaciation with a new mechanism for Bølling-Allerød warming. Science 325, 310–314.

Masson-Delmotte, V., Jouzel, J., Landais, A., Stievenard, M., Johnsen, S.J., White, J.W.C., Sveinbjornsdottir, A., Fuhrer, K., 2005. Deuterium excess reveals millennial and orbital scale fluctuations of Greenland moisture origin. Science 309, 118–121.

McManus, J.F., Francois, R., Gherardi, J.M., Keigwin, L.D., Brown-Leger, S., 2004. Collapse and rapid resumption of Atlantic meridional circulation linked to deglacial climate changes. Nature 428 (6985), 834–837.

Monson, R., Trahan, N., Rosenstiel, T., Veres, P., Moore, S.O., Wiklinson, M., Norby, R., Volder, A., Tjoelker, M., Briske, D., Karnosky, D., Fall, R., 2007. Isoprene emission from terrestrial ecosystems in response to global change: minding the gap between models and observations. Philos. Trans. R. Soc. A 365, 1677–1695.

Monteith, J.L., Unsworth, M.H., 1990. Principles of Environmental Physics. Academic Press, San Diego.

NGRIP Project Members, 2004. High-resolution record of Northern Hemisphere climate extending into the Last Interglacial period. Nature 431, 147–151.

Peltier, W., 2004. Global glacial isostasy and the surface of the ice age earth: the ICE-5G (VM2) model and GRACE. Annu. Rev. Earth Planet. Sci. 32, 111–1149.

Peterson, L.C., Haug, G.H., Hughen, K.A., Rohl, U., 2000. Rapid changes in the hydrologic cycle of the tropical Atlantic during the last glacial. Science 290, 1947–1951.

Possell, M., Hewitt, C., Beerling, D., 2005. The effects of glacial atmospheric CO_2 concentrations and climate on isoprene emissions by vascular plants. Glob. Change Biol. 1, 60–69.

Prather, M., Hsu, J., 2010. Coupling of nitrous oxide and methane by global atmospheric chemistry. Science 330, 952–954.

Randall, D., Wood, R., Bony, S., Colman, R., Fichefet, T., Fyfe, J., Kattsov, V., Pitman, A., Shukla, J., Srinivasan, J., Stouffer, R., Sumi, A., Taylor, K., 2007. Climate models and their evaluation. In: Solomon, S., Qin, D., Manning, M., Chen, Z., Marquis, M., Averyt, K.B., Tignor, M., Miller, H.L. (Eds.), Climate Change 2007: The Physical Science Basis: Contribution of Working Group I to the Fourth Assessment Report of the Intergovernmental Panel on Climate Change. C.U.P, Cambridge, U.K. and New York, U.S.A.

Ringeval, B., de Noblet-Ducoudre, N., Ciais, P., Bousquet, P., Prigent, C., Papa, F., Rossow, W., 2010. An attempt to quantify the impact of changes in wetland extent on methane emissions on the seasonal and interannual time scales. Glob. Biogeochem. Cycles 24 (GB2003).

Sanchez-Goñi, M.-F., Harrison, S., 2010. Millennial-scale climate variability and vegetation changes during the Last Glacial: concepts and terminology. Quaternary Sci. Rev. 29 (21–22), 2823–2827.

Schmittner, A.E., Galbraith, E.D., 2008. Glacial greenhouse gas fluctuations controlled by ocean circulation changes. Nature 456, 373–376.

Seager, R., Battisti, D.S., 2007. Challenges to our understanding of the general circulation: abrupt climate change. In: Lorenz, E.N., Schneider, T., Sobel, A.H. (Eds.), The Global Circulation of the Atmosphere. Princeton University Press, Princeton, U.S.A.

Singarayer, J., Valdes, P., 2010. High-latitude climate sensitivity to ice-sheet forcing over the last 120 kyr. Quaternary Sci. Rev. 29 (1–2), 43–55.

Singarayer, J., Valdes, P., Friedlingstein, P., Nelson, S., Beerling, D., 2011. Late Holocene methane rise caused by orbitally controlled increase in tropical sources. Nature 470, 82–85.

Smith, R., Gregory, J., 2009. A study of the sensitivity of ocean overturning circulation and climate to freshwater input in different regions of the North Atlantic. Geophys. Res. Lett. 36 (L15701).

Smith, R., Osprey, A., Gregory, J., 2008. A description of the FAMOUS (version XDBUA) climate model and control run. Geosci. Model Dev. 1, 53–68.

Stouffer, R.J., Yin, J., Gregory, J.M., Dixon, K.W., Spelman, M.J., Hurlin, W., Weaver, A.J., Eby, M., Flato, G.M., Hasumi, H., Hu, A., Jungclaus, J.H., Kamenkovich, I.V., Levermann, A., Montoya, M., Murakami, S., Nawrath, S., Oka, A., Peltier, W.R., Robitaille, D.Y., Sokolov, A., Vettoretti, G., Weber, S.L., 2006. Investigating the causes of the response of the thermohaline circulation to past and future climate changes. J. Clim. 19 (8), 1365–1387.

Swingedouw, D., Mignot, J., Braconnot, P., Mosquet, E., Kageyama, M., Alkama, R., 2009. Impact of freshwater release in the North Atlantic under different climate conditions in an OAGCM. J. Clim. 22, 6377–6403.

Timmermann, A., Okumura, Y., An, S.I., Clement, A., Dong, B., Guilyardi, E., Hu, A., J. H., J., Renold, M., Stocker, T., Stouffer, R.J., Sutton, R., Xie, R.-P., Yin, J., 2007. The influence of a weakening of the Atlantic Meridional overturning circulation on ENSO. J. Clim. 20, 4899–4918.

Valdes, P., Beerling, D., Johnson, C., 2005. The ice age methane budget. Geophys. Res. Lett. 32 (L02704).

Vellinga, M., Wood, R.A., 2002. Global climatic impacts of a collapse of the Atlantic thermohaline circulation. Clim. Change 54, 251–267.

Wang, X., Auler, A., Edwards, R., Cheng, H., Cristalli, P., Smart, P., Richards, D., Shen, C.-C., 2004. Wet periods in northeastern Brazil over the past 210 kyr linked to distant climate anomalies. Nature 432, 740–743.

Weber, S., Drury, A., Toonen, W., van Weele, M., 2010. Wetland methane emissions during the Last Glacial Maximum estimated from PMIP2 simulations: climate, vegetation, and geographic controls. J. Geophys. Res. 115 (D06111).

Wolff, E.W., Chappellaz, J., Blunier, T., Rasmussen, S.O., Svensson, A., 2010. Millennial-scale variability during the last glacial: the ice core record. Quaternary Sci. Rev. 29 (21–22), 2828–2838.

Woodward, F., Smith, T., Emanuel, W., 1995. A global land primary productivity and phytogeography model. Glob. Biogeochem. Cycles 9 (4), 471–490.

Wunsch, C., 2006. Abrupt climate change: an alternative view. Quaternary Sci. Rev. 65, 191–203.